

**Attosecond-Scale Streaking Methods for Strong-Field Ionization by Tailored Fields**Nicolas Eicke,<sup>\*</sup> Simon Brennecke, and Manfred Lein*Institut für Theoretische Physik, Leibniz Universität Hannover, Appelstraße 2, 30167 Hannover, Germany*

(Received 27 May 2019; published 29 January 2020)

Streaking with a weak probe field is applied to ionization in a two-dimensional strong field tailored to mimic linear polarization, but without disturbance by recollision or intracycle interference. This facilitates the observation of electron-momentum-resolved times of ionization with few-attosecond precision, as demonstrated by simulations for a model helium atom. Aligning the probe field along the ionizing field provides meaningful ionization times in agreement with the attoclock concept that ionization at maximum field corresponds to the peak of the momentum distribution, which is shifted due to the Coulomb force on the outgoing electron. In contrast, this attoclock shift is invisible in orthogonal streaking. Even without a probe field, streaking happens naturally along the laser propagation direction due to the laser magnetic field. As with an orthogonal probe field, the attoclock shift is not accessible by the magnetic-field scheme. For a polar molecule, the attoclock shift depends on orientation, but this does not imply an orientation dependence in ionization time.

DOI: [10.1103/PhysRevLett.124.043202](https://doi.org/10.1103/PhysRevLett.124.043202)

Measuring the time of ionization in weak- and strong-field ionization of atoms and molecules is an important aspect of light-matter interaction [1–3]. Apart from fundamental interest in the question of whether ionization maximizes at the peak of an applied strong field, there are wide-ranging practical implications because cornerstones of strong-field physics, such as high-harmonic generation (HHG) and high-energy above-threshold ionization, are often explained in terms of electron trajectories that depart from the atom at a well-defined time [4–6].

A frequently used tool to measure ionization times is known as attosecond angular streaking or the “attoclock.” There, an elliptically polarized laser field is used to map the ionization time of the photoelectron to its detection angle [7–18] (see also the recent work on atomic hydrogen [19]). A careful analysis is needed to retrieve the ionization time because Coulomb forces on the outgoing electron shift the peak of the photoelectron momentum distribution (PMD) with respect to naive modeling that predicts the peak at the negative vector potential of the driving field (“attoclock shift”). Ionization times in linear polarization, on the other hand, can be measured using two-color streaking schemes. The orthogonal two-color (OTC) scheme has been introduced for both HHG [20,21] and photoelectrons [22,23]. A weak orthogonal second-harmonic field was added to the strong driving field to deflect the electron trajectory after ionization. By observing the harmonic yield or PMD changing with the relative phase between the two colors, the ionization time (and recombination time in HHG) can be found. In the parallel two-color (PTC) scheme, the probe field is used to intervene into the ionization process directly, as the relative phase influences the total field strength of the combined field and hence the ionization rates. This gave access to ionization times of trajectories in

photoelectron holography [24] and is closely related to phase-of-the-phase spectroscopy [25,26].

Analyzing PTC data for linear polarization requires complicated modeling [24] because the electrons are strongly affected by the Coulomb force. Moreover, electrons launched during ascending quarter cycles of the field are inaccessible, as they are hidden under the dominating Coulomb-focused electrons launched after the field maximum, and in HHG, they do not contribute to the signal at all. Recently, we have proposed an alternative wave form as an ionizing field for studies of strong-field dynamics: A bicircular  $\omega$ - $2\omega$  field composed of two counterrotating components [27–30] can be tailored such that it approximates linear polarization three times per optical cycle of the fundamental component, while providing a time-to-momentum mapping similar to the attoclock [31]. Although ionization takes place as in a linearly polarized field, difficulties such as Coulomb focusing, intracycle interference, or rescattering [6,32–35] are avoided.

In this Letter, we combine the bicircular field with streaking, resulting in a method for ionization-time retrieval with few-attosecond precision, leading to several important findings. It gives us access to the region of peak field strength and the branch of trajectories originating during the ascending field, which could not be resolved in previous two-color schemes. In particular, we can compare the attoclock shift of the PMD with the momentum, at which time zero is found according to the streaking scheme, allowing us to connect two previously distinct notions of ionization time. We find that the PTC scheme yields results in excellent agreement with the attoclock shift, both for atoms and molecules, while the OTC scheme does not reveal the attoclock shift. We trace this discrepancy back to qualitatively different physical mechanisms: The OTC

scheme exploits the displacement of momentum-space structures by the streaking field, while in the PTC scheme the probe field modifies the ionization rate responsible for a given momentum. For molecules, our study sheds light on the question of whether the ionization time in a molecule depends on the electron emission direction—a question that was previously studied only for single-photon ionization [36–40], despite molecular attoclock setups already being considered [41–43]. Finally, motivated by a recent experiment [44], we attempt to exploit the dynamics beyond the electric-dipole approximation for attosecond time retrieval by considering the Lorentz force on the outgoing electron as a streaking force. This approach faces similar issues as the OTC scheme.

We solve the two-dimensional time-dependent Schrödinger equation (TDSE) using the split-operator method [45] with time step 0.006 a.u. on a Cartesian grid with 2048 points per dimension and box size  $400 \times 400$  a.u. The potential  $V(\mathbf{r}) = -1/\sqrt{\mathbf{r}^2 + \alpha}$  with  $\alpha \approx 0.0684$  a.u. reproduces the ionization potential  $I_p = 0.904$  a.u. of helium (atomic units are used unless stated otherwise). The PMD is obtained by projecting outgoing wave packets onto Volkov states using an absorber covering a distance of 50 a.u. from the boundary [46]. The vector potential [31]

$$\mathbf{A}(t) = -\frac{2}{\sqrt{5}} \frac{E_0}{\omega} \left[ \begin{pmatrix} \cos(\omega t) \\ \sin(\omega t) \end{pmatrix} + \frac{1}{4} \begin{pmatrix} -\cos(2\omega t) \\ \sin(2\omega t) \end{pmatrix} \right] \quad (1)$$

describes a counterrotating bicircular field  $\mathbf{E}(t) = -\dot{\mathbf{A}}(t)$ . With field-strength ratio 2:1 of the fundamental to second harmonic, the field resembles a linearly polarized field near its peaks with field strength  $E_{\text{peak}} = 3E_0/\sqrt{5}$  and effective frequency  $\omega_{\text{eff}} = \sqrt{2}\omega$ . Near  $t = 0$  we can write

$$\begin{aligned} \mathbf{A}_{\text{eff}}(t) &= A_x(0)\mathbf{e}_x - E_{\text{peak}}/\omega_{\text{eff}} \sin(\omega_{\text{eff}}t)\mathbf{e}_y \\ \mathbf{E}_{\text{eff}}(t) &= E_{\text{peak}} \cos(\omega_{\text{eff}}t)\mathbf{e}_y, \end{aligned} \quad (2)$$

with  $\mathbf{E}(t) = \mathbf{E}_{\text{eff}}(t) + \mathcal{O}(t^3)$ . We choose  $\omega_{\text{eff}} = 0.05695$  a.u. corresponding to 800 nm, so the actual wavelength of the fundamental field is 1131 nm. In addition to the bicircular field, we apply a weak linearly polarized streaking field via

$$\Delta\mathbf{A}(t, \phi) = -\epsilon E_{\text{peak}}/(2\omega_{\text{eff}}) \sin(2\omega_{\text{eff}}t + \phi)\mathbf{e}_i, \quad (3)$$

with relative phase  $\phi$ , effective frequency  $2\omega_{\text{eff}}$ , and relative field strength  $\epsilon = 0.02$ . Its polarization axis is  $\mathbf{e}_i = \mathbf{e}_x$  for orthogonal streaking or  $\mathbf{e}_i = \mathbf{e}_y$  for the parallel scheme. For the numerical calculations, the vector potentials (1) and (3) are multiplied with an envelope  $\cos(\omega t/6)^4$  (three-cycle pulse).

The momentum distribution at  $E_0 = 0.1$  a.u. without streaking field is shown in Fig. 1(a). It exhibits a main maximum corresponding to the region of almost linear

polarization around the peak of the pulse at  $t = 0$ . The maximum shows an attoclock shift in the positive  $p_y$  direction, see the projection in Fig. 1(b), which was investigated in [31].

The effect of the streaking field (3) on the momentum distribution can be understood within strong-field approximation (SFA). We wish to relate the optimal phase  $\bar{\phi}$  maximizing the signal at a given  $p_y$  to the ionization time. Motivated by the approximate vector potential (2), we write an action  $S_0$  from which the signal on the line  $p_x = -A_x(0)$  can be calculated,  $S_0(t_s, p_y) = -I_p t_s + \frac{1}{2} \int_{t_s}^T dt [p_y + A_y^{\text{eff}}(t)]^2$ . Here,  $t_s$  is the stationary point  $\partial S_0/\partial t_s = 0$ , and  $T$  is a time after the end of the pulse. The streaking vector potential (3) introduces a perturbation to the action. Since  $\Delta A_x$  and  $\Delta A_y$  are small, we neglect their contribution to the saddle-point time  $t_s$  and write  $S = S_0 + \Delta S_{\perp, \parallel}$  with  $\Delta S_{\perp} = \frac{1}{2} \int_{t_s}^T dt [\Delta A_x(t, \phi)]^2$  for orthogonal streaking and  $\Delta S_{\parallel} = \int_{t_s}^T dt [p_y + A_y^{\text{eff}}(t)] \Delta A_y(t, \phi)$  for the parallel scheme. For a given real part  $t_r = \text{Re} t_s$ , a maximum of the signal as a function of  $\phi$  is obtained when  $\partial_{\phi} \text{Im} \Delta S = 0$ . For orthogonal streaking, inserting the expressions (2) for  $A_y^{\text{eff}}$  and (3) for  $\Delta A_x$  leads to

$$\sin(2\omega_{\text{eff}}t_r + \bar{\phi}) = 0 \Rightarrow t_r = \frac{-\bar{\phi}}{2\omega_{\text{eff}}}. \quad (4)$$

This gives a direct relation between the observed relative phase  $\bar{\phi}$  and the time  $t_r$ , which we consider the physical ionization time. For the parallel scheme we find the condition  $2 \cos(\omega_{\text{eff}}t_r) \sin(2\omega_{\text{eff}}t_r + \bar{\phi}) = \cos(2\omega_{\text{eff}}t_r + \bar{\phi}) \times \sin(\omega_{\text{eff}}t_r)$ . This is satisfied by [47]

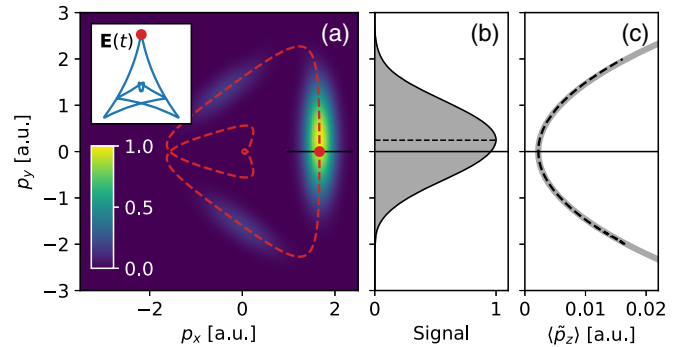


FIG. 1. (a) Momentum distribution for field strength  $E_0 = 0.10$  a.u. (intensity  $7 \times 10^{14}$  W/cm<sup>2</sup>). (Red dashed line) Negative vector potential. (Inset) Electric field. The red dot indicates  $t = 0$ . (b) Projection of the main branch of the PMD onto the  $p_y$  axis. (c)  $p_y$ -dependent nondipole shift  $\langle \tilde{p}_z \rangle = \langle p_z \rangle - p_x^2/(2c)$  on a line through the maximum of the 3D PMD (black dashed line) in comparison with the simple estimate (7) at  $\mathbf{v}_0 = 0$  (gray solid line). The value subtracted in the definition of  $\langle \tilde{p}_z \rangle$  accounts for the displacement of the momentum distribution in the  $p_x$  direction, which causes an additional nondipole shift compared to linear polarization.

$$t_r = \frac{4}{3} \frac{-\bar{\phi}}{2\omega_{\text{eff}}} + \mathcal{O}(\bar{\phi})^3, \quad (5)$$

where we will neglect the small higher-order terms. The potentially surprising factor of  $4/3$  is also obtained in a classical Coulomb-free model as a secondary effect of the streaking field when assuming that the signal at a given  $p_y$  goes through a maximum as a function of  $\phi$  when the total field at the time of ionization is maximized. Here, the probe field perturbs not only the field strength, but also the time-to-momentum mapping.

In practice, we do not use the straight line  $p_x = -A_x(0)$  in the OTC scheme. Instead, we start from the unperturbed momentum distribution [ $\epsilon = 0$ , Fig. 1(a)] and obtain a reference line by finding the maximum for every  $p_y$ . The streaking field changes the  $p_x$  position of the maximum. From the TDSE, we find for every  $p_y$  the optimal phase  $\bar{\phi}$  for which the maximum crosses the reference. For the PTC scheme, we project the main branch of the PMD onto the  $p_y$  axis, as in Fig. 1(b), and we observe for every  $p_y$  the yield as a function of  $\phi$ . The two schemes are illustrated in Fig. 2.

Our results are shown in Fig. 3, providing directly the ionization time for every momentum  $p_y$ . Negative times correspond to the rising slope of the ionizing field, which was inaccessible in previously implemented two-color schemes. In orthogonal streaking, the retrieved ionization time [Fig. 3(a), black solid line] agrees perfectly with the SFA saddle-point time, although the PMD (Fig. 1) shows a substantial attoclock shift of about  $\Delta p_y = 0.245$  a.u. The parallel scheme, in contrast, does reflect the attoclock shift [see the black line indicating maximal signal in Fig. 3(b)]. The shift is smaller for earlier ionization times, which is plausible because the Coulomb effect on the outgoing electron is less significant when the peak of the pulse is yet to come. At  $\bar{\phi} = 0$ , we find  $\Delta p_y = 0.255$  a.u. Orthogonal streaking gives only  $\Delta p_y = 0.015$  a.u.

Figure 4(a) shows the intensity dependence of the momenta with  $\bar{\phi} = 0$  (interpreted as time zero), in comparison with the attoclock shift obtained from the location of the PMD peak. It confirms the very good agreement

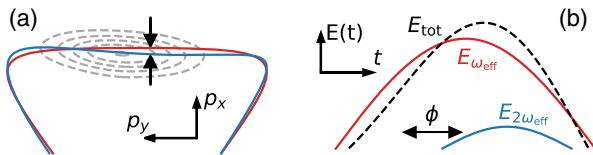


FIG. 2. Probing schemes (schematically,  $\phi \approx -1.0$ ). (a) OTC. Probe field along  $x$  displaces the negative vector potential (blue curve) and thus the PMD relative to the unstreaked reference (red curve). (b) PTC. Probe field along  $y$  modulates the total field strength (black dashed curve) and thus the ionization rate. In the relevant branch of the PMD, the modulation (Michelson contrast) is 18%, while in the orthogonal case it is negligible.

between parallel streaking and the attoclock shift. At high intensities, both observables begin to reflect the depletion of the bound state and the agreement slightly diminishes. Orthogonal streaking, on the other hand, always gives values near zero. These results lead to our main conclusion that the PTC scheme is consistent with the attoclock concept that time zero corresponds to the maximum of the PMD, while this is not true for the OTC scheme.

To explain this behavior, we first note that the PMD peak is located on the curve  $-\mathbf{A}$  with amazing accuracy, despite Coulomb forces and depletion (see Fig. 1). Apparently, these effects cause momentum shifts pointing along the curve  $-\mathbf{A}$ , not away from it. This is intuitive, as we ionize at times when the field is approximately linearly polarized so that its direction remains constant while the electron moves out; in such a symmetric situation, any momentum shift due to Coulomb forces or depletion must point along the symmetry axis given by  $\mathbf{E} = -\dot{\mathbf{A}}$ , i.e., along the curve  $-\mathbf{A}$ . (In addition, shifts due to nonadiabatic initial velocities are negligible near the peak, because both ionizing and probe fields vary slowly as they are close to their local maxima). Because of this, at  $p_y = 0$  the OTC scheme boils down to finding the optimal phase such that the probe field leaves the vector potential unchanged. This requires  $\phi = 0$ , implying via Eq. (4) that  $t_r = 0$  is assigned to  $p_y = 0$ . In an alternative view, the OTC scheme is not able to measure the true ionization time because the Coulomb interaction is neglected in the derivation of the phase-to-time mapping, which depends on the propagation step. In retrospect, this may explain why in [21] the ionization times retrieved from

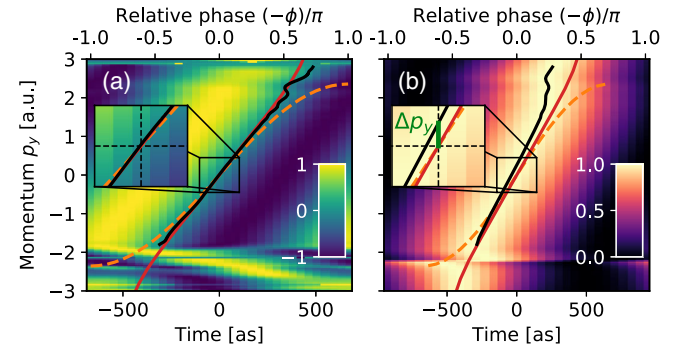


FIG. 3. (a) Orthogonal streaking. The color indicates the distance between the  $p_x$  position of the PMD maximum and the reference position, normalized for every  $p_y$  individually to maximum absolute value 1. The black solid line gives the relative phase where the maximum crosses the reference. Relative phase is converted to time via Eq. (4). (b) Parallel streaking. The color indicates the observed signal, integrated along  $p_x$  and normalized separately for each  $p_y$  to vary between zero and one. The black line gives the relative phase where the signal is maximized. Relative phase is converted to time via Eq. (5). In both panels, the real part of the SFA saddle-point time is shown as red solid line. The ionization time from the classical Coulomb-free model [ $\mathbf{p} = -\mathbf{A}_{\text{eff}}(t)$ ] is shown as orange dashed line.

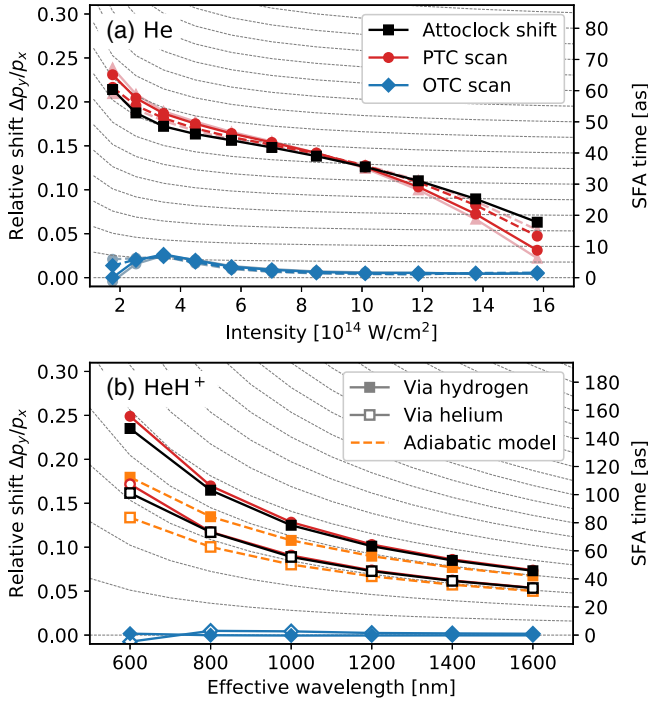


FIG. 4. (a) Momenta corresponding to  $\vec{\phi} = 0$  (interpreted as time zero) according to the OTC and PTC scans for the He model in comparison with attoclock shifts of the PMD. The dashed lines show the result when the streaking field is shifted by  $\phi = \pi$  and minimization is used instead of maximization in the case of the PTC scan. Light colors show results for larger probe field strength ( $\epsilon = 0.04$ ). (b) Orientation-dependent attoclock shifts and momenta corresponding to time zero for the HeH<sup>+</sup> model: filled symbols, ionization via H; open symbols, ionization via He; color coding as above. Here, we have combined the two streaking results for  $\phi$  and  $\phi + \pi$  into one by taking the average. Orange dashed lines, relative shift according to the adiabatic model, see text. For easy conversion to time, the SFA ionization times are shown as gray lines in the background of both panels.

the HHG-based OTC method are in such excellent agreement with SFA ionization times, although a Coulomb correction to ionization times similar to the attoclock shift is present also in HHG [48]. We conclude that OTC could measure the phase of the probe field on an absolute scale rather than true ionization times.

The PTC phase-to-time mapping exploits the enhancement of ionization by the probe field and it is hardly affected by Coulomb effects during propagation. The good agreement of the time-zero momenta with the attoclock shifts is consistent with the observation that the additional total yield due to a perturbing field is maximized when the peaks of perturbing and fundamental fields coincide [49]. Our Letter shows that not only is the overall yield maximized in this way, but also the signal at the PMD maximum. In particular, parallel streaking does not reproduce the delay of approximately 10 as found from an integral representation to define ionization time [31,50].

For both OTC and PTC schemes, the same conclusions are obtained when a  $2\omega$  or  $3\omega$  streaking field is used instead of  $2\omega_{\text{eff}}$ . Thus, in the range of frequencies considered, non-adiabatic effects in the probe field are irrelevant.

We can use the bicircular field to probe orientation-dependent properties of molecules. We consider an asymmetric potential

$$V(\mathbf{r}) = \frac{-1}{\sqrt{(\mathbf{r}-\mathbf{r}_1)^2 + 1/2}} + \frac{-(1 + e^{-\beta(\mathbf{r}-\mathbf{r}_2)^2})}{\sqrt{(\mathbf{r}-\mathbf{r}_2)^2 + 1/2}}, \quad (6)$$

with  $\beta = 1.063$  a.u. chosen to reproduce the ionization potential of HeH<sup>+</sup> (1.66 a.u.) at its equilibrium distance  $|\mathbf{r}_1 - \mathbf{r}_2| = 1.4$  a.u. [51]. We interpret  $\mathbf{r}_1$  as the location of the proton. We solve the 2D TDSE for the molecule oriented along or against the  $y$  axis at  $E_0 = 0.18$  a.u. and various wavelengths. We find that the attoclock shift depends on the orientation [see Fig. 4(b)]. The PTC scan shows good agreement between the attoclock shift and the momenta of time zero for both orientations, suggesting that the orientation dependence of the attoclock shift does not correspond to a real delay in ionization time. For the ionization-time difference between the two orientations, we find numbers below 1.5 as. Indeed, the shift can be understood in an adiabatic model without such a delay. By solving the Schrödinger equation for the molecule in the static external field  $E$ , we find  $I_p(E) = 1.657 + 0.403E + 0.633E^2$ . This change in  $I_p$  leads to an orientation-dependent change of the tunnel-exit position obtained from 2D parabolic coordinates [9,17]. We solve Newton's equation of motion in a static field with  $V(r) = -2/r$ , starting from the tunnel exit with zero velocity. Then we evaluate  $\Delta p = p(t) - p_0(t)$  for large  $t$ , where  $p(t)$  is the time-dependent momentum and  $p_0(t)$  is the momentum assuming  $V = 0$ . The result [orange curves in Fig. 4(b)] shows good agreement for long wavelengths.

A transverse force on outgoing electrons is realized not only with a streaking field; such a force is inherently present because of the magnetic component of the laser pulse [52–54]. It causes a momentum transfer in the light-propagation direction that varies on a subcycle timescale [44]. The point of minimal momentum transfer defines a reference that one might be tempted to identify as the time of peak field. We solve the 3D TDSE including nondipole effects to first order in  $1/c$  [54,55], using an effective potential [56] for helium converted into a pseudopotential for the  $1s$  state at cutoff radius  $r_{cl} = 1.5$  a.u. [57]. The  $p_y$ -dependent nondipole shift  $\langle p_z \rangle$  is shown in Fig. 1(c). Assuming Coulomb-free classical motion starting with velocity  $\mathbf{v}_0$  after tunnel ionization, this shift can be modeled as

$$\langle p_z \rangle \approx \frac{2I_p + \mathbf{v}_0^2}{6c} + \frac{\mathbf{p}^2}{2c} - \frac{\mathbf{v}_0^2}{2c}. \quad (7)$$

The first term arises from the magnetic field during tunneling [58,59]. The last two terms correspond to the energy gained after tunneling, divided by  $c$ . We find almost perfect agreement with the TDSE. In particular, the point of minimal nondipole shift corresponds to  $p_y \approx 0$  rather than the PMD maximum. A similar discrepancy was observed experimentally in elliptical polarization [44]. Since the nondipole shift is acquired during the entire pulse but the attoclock shift  $\Delta p_y$  is acquired during a short time after tunneling, we can view the Coulomb influence as an initial velocity offset  $\mathbf{v}_0 = \Delta p_y \mathbf{e}_y$  in the last term of Eq. (7). This affects the magnitude of the nondipole shift, but not the momentum at which the minimal shift occurs. Finite-time corrections to this short-kick picture are only weakly momentum dependent. Hence, it is inaccurate to identify minimal nondipole shift with time zero. Instead, it provides the location of  $p_y = 0$  in an experiment where the bicircular-field orientation is unknown.

To conclude, we have compared several experimentally feasible approaches to extract attosecond-precision strong-field dynamics from photoelectron distributions. A weak probe field polarized along the ionizing field gives results confirming that ionization occurs most likely at the highest instantaneous field. This remains valid for polar molecules, implying nearly orientation-independent ionization times. Streaking outgoing electrons orthogonal to the ionizing field, either by an external field or by the magnetic component of the ionizing field, measures ionization time as if the outgoing electron did not feel the Coulomb force. The parallel approach is free of these complications and we expect it is transferable to electron emission from other systems of scientific interest such as nanotips [60,61] and liquids [62].

This work has been supported by the Deutsche Forschungsgemeinschaft through the Priority Programme *Quantum Dynamics in Tailored Intense Fields* (QUTIF).

---

\* nicolas.eicke@itp.uni-hannover.de

- [1] J. M. Dahlström, A. L'Huillier, and A. Maquet, Introduction to attosecond delays in photoionization, *J. Phys. B* **45**, 183001 (2012).
- [2] A. N. Pfeiffer, C. Cirelli, M. Smolarski, and U. Keller, Recent attoclock measurements of strong field ionization, *Chem. Phys.* **414**, 84 (2013).
- [3] A. S. Landsman and U. Keller, Attosecond science and the tunnelling time problem, *Phys. Rep.* **547**, 1 (2015).
- [4] J. L. Krause, K. J. Schafer, and K. C. Kulander, High-Order Harmonic Generation from Atoms and Ions in the High Intensity Regime, *Phys. Rev. Lett.* **68**, 3535 (1992).
- [5] P. B. Corkum, Plasma Perspective on Strong Field Multiphoton Ionization, *Phys. Rev. Lett.* **71**, 1994 (1993).
- [6] G. G. Paulus, W. Nicklich, H. Xu, P. Lambropoulos, and H. Walther, Plateau in above Threshold Ionization Spectra, *Phys. Rev. Lett.* **72**, 2851 (1994).
- [7] P. Eckle, M. Smolarski, P. Schlup, J. Biegert, A. Staudte, M. Schöffler, H. G. Muller, R. Dörner, and U. Keller, Attosecond angular streaking, *Nat. Phys.* **4**, 565 (2008).
- [8] P. Eckle, A. N. Pfeiffer, C. Cirelli, A. Staudte, R. Dörner, H. G. Muller, M. Büttiker, and U. Keller, Attosecond ionization and tunneling delay time measurements in helium, *Science* **322**, 1525 (2008).
- [9] A. N. Pfeiffer, C. Cirelli, M. Smolarski, D. Dimitrovski, M. Abu-samha, L. B. Madsen, and U. Keller, Attoclock reveals natural coordinates of the laser-induced tunnelling current flow in atoms, *Nat. Phys.* **8**, 76 (2012).
- [10] A. S. Landsman, M. Weger, J. Maurer, R. Boge, A. Ludwig, S. Heuser, C. Cirelli, L. Gallmann, and U. Keller, Ultrafast resolution of tunneling delay time, *Optica* **1**, 343 (2014).
- [11] L. Torlina, F. Morales, J. Kaushal, I. Ivanov, A. Kheifets, A. Zielinski, A. Scrinzi, H. G. Muller, S. Sukiasyan, M. Ivanov, and O. Smirnova, Interpreting attoclock measurements of tunnelling times, *Nat. Phys.* **11**, 503 (2015).
- [12] M. Klaiber, K. Z. Hatsagortsyan, and C. H. Keitel, Tunneling Dynamics in Multiphoton Ionization and Attoclock Calibration, *Phys. Rev. Lett.* **114**, 083001 (2015).
- [13] N. Camus, E. Yakaboylu, L. Fechner, M. Klaiber, M. Laux, Y. Mi, K. Z. Hatsagortsyan, T. Pfeifer, C. H. Keitel, and R. Moshhammer, Experimental Evidence for Quantum Tunneling Time, *Phys. Rev. Lett.* **119**, 023201 (2017).
- [14] V. P. Majety and A. Scrinzi, Absence of electron correlation effects in the helium attoclock setting, *J. Mod. Opt.* **64**, 1026 (2017).
- [15] H. Ni, U. Saalman, and J. M. Rost, Tunneling Ionization Time Resolved by Backpropagation, *Phys. Rev. Lett.* **117**, 023002 (2016).
- [16] H. Ni, U. Saalman, and J. M. Rost, Tunneling exit characteristics from classical backpropagation of an ionized electron wave packet, *Phys. Rev. A* **97**, 013426 (2018).
- [17] H. Ni, N. Eicke, C. Ruiz, J. Cai, F. Oppermann, N. I. Shvetsov-Shilovski, and L. W. Pi, Tunneling criteria and a nonadiabatic term for strong-field ionization, *Phys. Rev. A* **98**, 013411 (2018).
- [18] M. Han, P. Ge, Y. Fang, X. Yu, Z. Guo, X. Ma, Y. Deng, Q. Gong, and Y. Liu, Unifying Tunneling Pictures of Strong-Field Ionization with an Improved Attoclock, *Phys. Rev. Lett.* **123**, 073201 (2019).
- [19] U. S. Sainadh, H. Xu, X. Wang, A. Atia-Tul-Noor, W. C. Wallace, N. Douguet, A. Bray, I. Ivanov, K. Bartschat, A. Kheifets, R. T. Sang, and I. V. Litvinyuk, Attosecond angular streaking and tunnelling time in atomic hydrogen, *Nature (London)* **568**, 75 (2019).
- [20] D. Shafir, H. Soifer, B. D. Bruner, M. Dagan, Y. Mairesse, S. Patchkovskii, M. Y. Ivanov, O. Smirnova, and N. Dudovich, Resolving the time when an electron exits a tunnelling barrier, *Nature (London)* **485**, 343 (2012).
- [21] J. Zhao and M. Lein, Determination of Ionization and Tunneling Times in High-Order Harmonic Generation, *Phys. Rev. Lett.* **111**, 043901 (2013).
- [22] J. Henkel and M. Lein, Analysis of electron trajectories with two-color strong-field ionization, *Phys. Rev. A* **92**, 013422 (2015).
- [23] N. Eicke and M. Lein, Extracting trajectory information from two-color strong-field ionization, *J. Mod. Opt.* **64**, 981 (2017).

- [24] G. Porat, G. Alon, S. Rozen, O. Pedatzur, M. Krüger, D. Azoury, A. Natan, G. Orenstein, B. D. Bruner, M. J. J. Vrakking, and N. Dudovich, Attosecond time-resolved photoelectron holography, *Nat. Commun.* **9**, 2805 (2018).
- [25] S. Skruszewicz, J. Tiggesbäumker, K. H. Meiwes-Broer, M. Arbeiter, T. Fennel, and D. Bauer, Two-Color Strong-Field Photoelectron Spectroscopy and the Phase of the Phase, *Phys. Rev. Lett.* **115**, 043001 (2015).
- [26] V. A. Tulsy, M. A. Almajid, and D. Bauer, Two-color phase-of-the-phase spectroscopy with circularly polarized laser pulses, *Phys. Rev. A* **98**, 053433 (2018).
- [27] H. Eichmann, A. Egbert, S. Nolte, C. Momma, B. Wellenhausen, W. Becker, S. Long, and J. K. McIver, Polarization-dependent high-order two-color mixing, *Phys. Rev. A* **51**, R3414 (1995).
- [28] D. B. Milošević and W. Becker, Attosecond pulse trains with unusual nonlinear polarization, *Phys. Rev. A* **62**, 011403(R) (2000).
- [29] O. Kfir, P. Grychtol, E. Turgut, R. Knut, D. Zusin, D. Popmintchev, T. Popmintchev, H. Nembach, J. M. Shaw, A. Fleischer, H. Kapteyn, M. Murnane, and O. Cohen, Generation of bright phase-matched circularly-polarized extreme ultraviolet high harmonics, *Nat. Photonics* **9**, 99 (2015).
- [30] D. B. Milošević and W. Becker, Improved strong-field approximation and quantum-orbit theory: Application to ionization by a bicircular laser field, *Phys. Rev. A* **93**, 063418 (2016).
- [31] N. Eicke and M. Lein, Attoclock with counter-rotating bicircular laser fields, *Phys. Rev. A* **99**, 031402(R) (2019).
- [32] A. Rudenko, K. Zrost, T. Ergler, A. B. Voitkiv, B. Najjari, V. L. B. de Jesus, B. Feuerstein, C. D. Schröter, R. Moshhammer, and J. Ullrich, Coulomb singularity in the transverse momentum distribution for strong-field single ionization, *J. Phys. B* **38**, L191 (2005).
- [33] D. Comtois, D. Zeidler, H. Pépin, J. C. Kieffer, D. M. Villeneuve, and P. B. Corkum, Observation of Coulomb focusing in tunnelling ionization of noble gases, *J. Phys. B* **38**, 1923 (2005).
- [34] D. G. Arbó, E. Persson, and J. Burgdörfer, Time double-slit interferences in strong-field tunneling ionization, *Phys. Rev. A* **74**, 063407 (2006).
- [35] F. Lindner, M. G. Schätzel, H. Walther, A. Baltuška, E. Goulielmakis, F. Krausz, D. B. Milošević, D. Bauer, W. Becker, and G. G. Paulus, Attosecond Double-Slit Experiment, *Phys. Rev. Lett.* **95**, 040401 (2005).
- [36] A. Chacon, M. Lein, and C. Ruiz, Asymmetry of Wigner's time delay in a small molecule, *Phys. Rev. A* **89**, 053427 (2014).
- [37] P. Hockett, E. Frumker, D. M. Villeneuve, and P. B. Corkum, Time delay in molecular photoionization, *J. Phys. B* **49**, 095602 (2016).
- [38] M. Huppert, I. Jordan, D. Baykusheva, A. von Conta, and H. J. Wörner, Attosecond Delays in Molecular Photoionization, *Phys. Rev. Lett.* **117**, 093001 (2016).
- [39] D. Baykusheva and H. J. Wörner, Theory of attosecond delays in molecular photoionization, *J. Chem. Phys.* **146**, 124306 (2017).
- [40] J. Vos, L. Cattaneo, S. Patchkovskii, T. Zimmermann, C. Cirelli, M. Lucchini, A. Kheifets, A. S. Landsman, and U. Keller, Orientation-dependent stereo Wigner time delay and electron localization in a small molecule, *Science* **360**, 1326 (2018).
- [41] V. V. Serov, A. W. Bray, and A. S. Kheifets, Numerical attoclock on atomic and molecular hydrogen, *Phys. Rev. A* **99**, 063428 (2019).
- [42] V. Hanus, S. Kangaparambil, S. Larimian, X. Xie, M. Schöffler, A. Staudte, G. Paulus, A. Baltuska, and M. Kitzler, The molecular attoclock: Sub-cycle control of electronic dynamics during H<sub>2</sub> double ionization, *EPJ Web Conf.* **205**, 02002 (2019).
- [43] W. Quan, V. V. Serov, M. Z. Wei, M. Zhao, Y. Zhou, Y. L. Wang, X. Y. Lai, A. S. Kheifets, and X. J. Liu, Attosecond Molecular Angular Streaking with All-Ionic Fragments Detection, *Phys. Rev. Lett.* **123**, 223204 (2019).
- [44] B. Willenberg, J. Maurer, B. W. Mayer, and U. Keller, Sub-cycle time resolution of multi-photon momentum transfer in strong-field ionization, *Nat. Commun.* **10**, 5548 (2019).
- [45] M. D. Feit, J. A. Fleck, and A. Steiger, Solution of the Schrödinger equation by a spectral method, *J. Comput. Phys.* **47**, 412 (1982).
- [46] M. Lein, E. K. U. Gross, and V. Engel, Intense-Field Double Ionization of helium: Identifying the Mechanism, *Phys. Rev. Lett.* **85**, 4707 (2000).
- [47] For the short pulse used here, from the classical argument we find an additional factor of 27/26. Experimental implementation with  $2\omega_{\text{eff}} \approx 2.83\omega$  is challenging. Alternatively, using a  $2\omega$  or  $3\omega$  streaking field, the conversion (5) can be used when replacing  $2\omega_{\text{eff}} \rightarrow 2\omega$  and  $4/3 \rightarrow 2$  or  $2\omega_{\text{eff}} \rightarrow 3\omega$  and  $4/3 \rightarrow 9/7$ .
- [48] L. Torlina and O. Smirnova, Coulomb time delays in high harmonic generation, *New J. Phys.* **19**, 023012 (2017).
- [49] I. A. Ivanov, C. Hofmann, L. Ortmann, A. S. Landsman, C. H. Nam, and K. T. Kim, Instantaneous ionization rate as a functional derivative, *Commun. Phys.* **1**, 81 (2018).
- [50] N. Eicke and M. Lein, Trajectory-free ionization times in strong-field ionization, *Phys. Rev. A* **97**, 031402(R) (2018).
- [51] T. A. Green, H. H. Michels, J. C. Browne, and M. M. Madsen, Configuration interaction studies of the HeH<sup>+</sup> molecular ion. I Singlet sigma states, *J. Chem. Phys.* **61**, 5186 (1974).
- [52] C. T. L. Smeenk, L. Arissian, B. Zhou, A. Mysyrowicz, D. M. Villeneuve, A. Staudte, and P. B. Corkum, Partitioning of the Linear Photon Momentum in Multiphoton Ionization, *Phys. Rev. Lett.* **106**, 193002 (2011).
- [53] A. Ludwig, J. Maurer, B. W. Mayer, C. R. Phillips, L. Gallmann, and U. Keller, Breakdown of the Dipole Approximation in Strong-Field Ionization, *Phys. Rev. Lett.* **113**, 243001 (2014).
- [54] A. Hartung, S. Eckart, S. Brennecke, J. Rist, D. Trabert, K. Fehre, M. Richter, H. Sann, S. Zeller, K. Henrichs, G. Kastirke, J. Hoehl, A. Kalinin, M. S. Schöffler, T. Jahnke, L. P. H. Schmidt, M. Lein, M. Kunitski, and R. Dörner, Magnetic fields alter strong-field ionization, *Nat. Phys.* **15**, 1222 (2019).
- [55] S. Brennecke and M. Lein, High-order above-threshold ionization beyond the electric dipole approximation: Dependence on the atomic and molecular structure, *Phys. Rev. A* **98**, 063414 (2018).

- [56] X. M. Tong and C. D. Lin, Empirical formula for static field ionization rates of atoms and molecules by lasers in the barrier-suppression regime, *J. Phys. B* **38**, 2593 (2005).
- [57] N. Troullier and J. L. Martins, Efficient pseudopotentials for plane-wave calculations, *Phys. Rev. B* **43**, 1993 (1991).
- [58] M. Klaiber, E. Yakaboylu, H. Bauke, K. Z. Hatsagortsyan, and C. H. Keitel, Under-the-Barrier Dynamics in Laser-Induced Relativistic Tunneling, *Phys. Rev. Lett.* **110**, 153004 (2013).
- [59] S. Chelkowski, A. D. Bandrauk, and P. B. Corkum, Photon Momentum Sharing between an Electron and an Ion in Photoionization: From One-Photon (Photoelectric Effect) to Multiphoton Absorption, *Phys. Rev. Lett.* **113**, 263005 (2014).
- [60] H. Yanagisawa, S. Schnepp, C. Hafner, M. Hengsberger, D. E. Kim, M. F. Kling, A. Landsman, L. Gallmann, and J. Osterwalder, Delayed electron emission in strong-field driven tunnelling from a metallic nanotip in the multi-electron regime, *Sci. Rep.* **6**, 35877 (2016).
- [61] L. Seiffert, T. Paschen, P. Hommelhoff, and T. Fennel, High-order above-threshold photoemission from nanotips controlled with two-color laser fields, *J. Phys. B* **51**, 134001 (2018).
- [62] I. Jordan, M. Huppert, M. A. Brown, J. A. van Bokhoven, and H. J. Wörner, Photoelectron spectrometer for attosecond spectroscopy of liquids and gases, *Rev. Sci. Instrum.* **86**, 123905 (2015).